CHAPTER IV

THE APPLICATIONS

4.1 Introduction

The Neural Network control techniques have an ability to cater to the nonlinearity and complexity of processes without knowing the relation between inputs and outputs. The recent upsurge in neural network control research, (A. K. A. Wahub, M. A. Hussain and M. Z. Sulaiman, 2000; M.A. Hussain and L.S. Kershenbaum, 2000; N. Aziz, M. A. Hussain and I. M. Mujtaba, 2000; P. Kittisupakorn, M. A. Hussain and J. Petcherdsak, 2001), for example, had done much prior works on neural network already. However, those investigations did not apply the hybrid reactor. Moreover, the purpose of those previous researches were to control the reactor temperature for obtaining good productivity and the desired products, which can not guaranteed the control objective especially in cases of plant-model mismatches and disturbance changes. The purpose of this research is to control the reactant concentration in the reactor by manipulating the jacket set point temperature to obtain a high yield of the desired product. The product concentration set point is as much as possible; therefore, the certain product concentration set point is unavailable.

In this research, a Neural Network control strategy is designed and used for set point tracking and disturbances rejection in both nominal and plant-model mismatch conditions, compared with the conventional PID control.

This chapter describe all the procedures how to execute the given conundrum, "A Neural Network Modeling and Control for Etherification Hybrid Process", these applications are based on the theory introduced previously in CHAPTER III and some additionally more in this chapter and the appendices.

4.2 Hybrid Etherification Process

This is a combined process, using a Continuous Stirred Tank Reactor (CSTR), a Pervaporative Membrane Unit and a Heat Jacket for temperature adjustment.

Every species, except for the product, are separated while the reaction takes place, which causes the product to shift to higher levels of quantity and quality. The process schematic diagram is shown in Figure4.1.

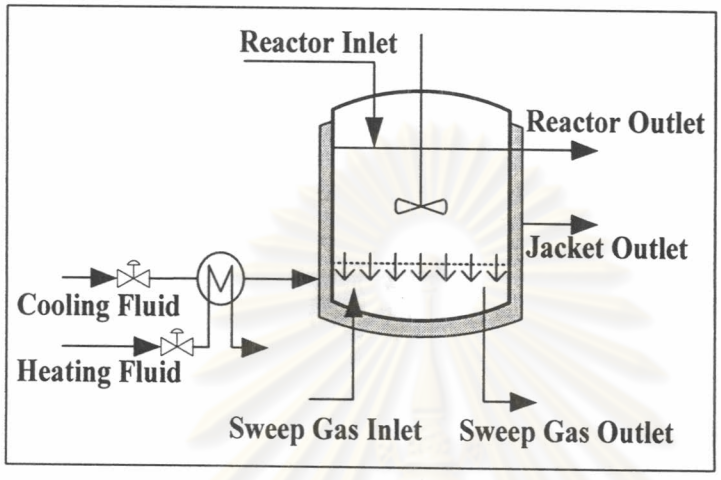

Figure 4.1: Process Schematic Diagram

The reactions in the reactor are recation1, which is a reversible reaction, and reaction2, which is an irreversible reaction as follow:

Reaction 1: $A + B \leftrightarrow P + W$

Reaction 2: $A \longrightarrow C + W$

Where

A represents TBA, reactant

B represents Ethanol, reactant

C represents Isobutene, by-product

P represents ETBE, desired product

W represents Water, by-product

4.2.1 White Box Mathematical Model

The white box mathematical model of the process is derived from Material Balance and Energy Balance equations. This supposes to be a real plant for simulation, under the following assumptions:

1. Concentration and temperature are distributed uniformly both in the reactor and the jacket.

2. The permeation of P is negligible (Assabumrungrat, 2003).

3. The amount of heat retained in the reactor walls is negligible compared to the heat transferred in the reactor.

Under the assumption above, the energy and material balance equations can be written as follows:

$$V\frac{dC_A}{dt} = F_v C_{Ain} - F_v C_A - AP_A a_A - W(r_1 + r_2) \tag{4.2}$$

$$V\frac{dC_B}{dt} = F_v C_{Bin} - F_v C_B - AP_B a_B - W(r_1) \tag{4.3}$$

$$V\frac{dC_P}{dt} = -F_v C_P + W(r_1) \tag{4.4}$$

$$V\frac{dC_W}{dt} = -F_v C_W - AP_W a_W + W(r_1 + r_2) \tag{4.5}$$

$$\frac{dT_r}{dt} = \frac{Q + UA(T_j - T_r)}{M_t C_{pt}} + \frac{F_v}{V}(T_F - T_r) \tag{4.6}$$

$$\frac{dT_j}{dt} = \frac{q_j \rho_j Cp_j (T_{jsp} - T_j) - UA(T_j - T_r)}{V_j \rho_j Cp_j} \tag{4.7}$$

The rate of the reactions and kinetic parameters can be expressed as follows:

$$r_1 = k_1 \frac{a_A a_B - a_P a_W / K_1}{1 + K_W a_W} \tag{4.7}$$

$$r_2 = k_2 \frac{a_A}{1 + K_W a_W} \tag{4.8}$$

$$k_1 = \exp\left(3.55 - \frac{2286}{T_r}\right) \tag{4.9}$$

$$k_2 = \exp\left(36.57 - \frac{13653}{T_r}\right) \tag{4.10}$$

$$K_W = \exp\left(-16.16 + \frac{6636}{T_r}\right) \tag{4.11}$$

$$K_i = \exp\left(1140 - \frac{14580}{T_r} + 232.9\ln T_r + 1.087 T_r \right.$$
$$\left. -1.114\times10^{-3} T_r^{\,2} + 5.538\times10^{-7} T_r^{\,3}\right) \tag{4.12}$$

The activities can be calculated from the following relationship:

$$a_i = \gamma_i x_i \tag{4.13}$$

γ_i, the activity coefficient can be estimated by using UNIFAC method.

The permeability coefficients can be expressed as follows:

$$P_A = \exp\left(7.67 - \frac{6434}{T_r}\right) \tag{4.14}$$

$$P_B = \exp\left(3.25 - \frac{4328}{T_r}\right) \tag{4.15}$$

$$P_W = \exp\left(2.07 - \frac{2441}{T_r}\right) \tag{4.16}$$

The total heat capacity can be expressed as follows:

$$C_{pt} = \frac{C_{pA}C_A + C_{pB}C_B + C_{pP}C_P + C_{pW}C_W}{C_A + C_B + C_P + C_W} \tag{4.17}$$

Where C_{pA}, C_{pB}, and C_{pW} are obtained from Perry's Chemical Engineer's Handbook, C_{pP} is calculated by these method:

- JOHN GARVIN liquid heat capacity: More details can be found in (John Garvin, 2002).

- JOBACK, critical temperature and normal boiling point: More details can be found in (Dragon Technology, 1995).

M_t and x_i can be calculated by the concentration of each species and reactor volume.

The heat released from reactions, Q, is the summation of heats from reaction1 and reaction2 which are estimated by:

$$Q_1 = W^* r_1 * \Delta H_1 \quad (4.18)$$

$$Q_2 = W^* r_2 * \Delta H_2 \quad (4.19)$$

Where, Q_1 is the heat released from reaction1

Q_2 is the heat released from reaction2

ΔH_1 is the heat of reaction 1

ΔH_2 is the heat of reaction 2

The heats of reactions are calculated by the summation of heats of formations of each species in reaction, heats of formations of each species are calculated by the following equation:

$$\Delta H_{F_i} = \Delta H_{F_i}^{298} + \int_{298}^{T} C_{p_i} dT \quad (4.20)$$

Where, ΔH_{Fi} is the heat of formation of specie *i*

ΔH_{Fi}^{298} is the standard heat of formation of specie *i* at 298 K

C_{Pi} is the heat capacity of specie *i*

The standard heats of formations of species A, B and W are obtain from Perry's Chemical Engineer's Handbook. The standard heat of formation of specie P is estimated by Joback's method (Dragon Technology, 1995).

4.2.2 Nominal Operating Condition

The operating condition for the nominal case simulation is shown as follows:

$A = 0.18\ [m^2]$

$C_A = 4.00 \times 10^3\ [mol/m^3]$

$C_B = 3.85 \times 10^3\ [mol/m^3]$

$C_P = 2.51 \times 10^3\ [mol/m^3]$

$C_W = 0.17 \times 10^3\ [mol/m^3]$

$C_{Ain} = 6.6 \times 10^3\ [mol/m^3]$

$C_{Bin} = 6.6 \times 10^3\ [mol/m^3]$

$F_v = 5 \times 10^{-6}\ [m^3/s]$

$q_j = 2.8 \times 10^{-7}\ [m^3/s]$

$T_F = 303\ [K]$

$T_j = 303\ [K]$

$T_{jsp} = 303\ [K]$

T_r = 303 [K]

UA = 6.25 [J/(s K)]

V = 3.6×10^{-4} [m^3]

V_j = 5×10^{-6} [m^3]

W = 3.96×10^{-2} [kg]

4.2.3 Process Analysis

In some cases, the material balance and energy balance equations are not available. In these cases, the white box model based controllers can not be used. The black box model based control strategies (Neural Network) is used in this research compared with the non-model based (conventional PID).

Control Objective: Maximum Product

Inputs: C_{Ain}, C_{Bin}, q_j, T_j, T_F

Outputs: C_A, C_B, C_P, C_W, T_r

4.2.3.1 Controlled Variable Selection

- T_r can not guarantee the control objective especially in cases of disturbance change.

- C_W is not related to the control objective, either high or low values of C_W do not correspond to a large value of C_P.

- C_P is directly related to the control objective, but the set point is unavailable.

- C_A and C_B, the reactants concentrations, are indirectly related to the control objective. The set point is available by setting to a small value.

Considering C_A, the small value of it can be caused by:

1. high rate of both reaction1 and reaction2

2. high permeation rate of the by product (Water), which can cause high rate of both reactions

3. high permeation rate of A

Considering C_B, the small value of it can be caused by:

1. high rate of reaction1

2. high permeation rate of the by product (Water), which can cause a high rate of both reactions

3. high permeation rate of B

From these causes, C_B can guarantee the control objective better than C_A, because C_A can be decreased by the side reaction, but the product is not occurred from this. Also, in case of a high permeation rate of B, the permeated can be recycled back or else, the permeation rate of B can be impeded by the increase of the vapor pressure of B in the permeated side. Therefore, the best controlled variable for this process is C_B.

4.2.3.2 Manipulated Variable Selection

- Considering T_F, it has many disadvantages for adjusting the temperature, which are; the heat transfer rate is limited by the constant reactor feed flow rate, the temperature manipulating range is limited by the reactants phase changes, the side reaction of each individual reactant may occur without producing the product.

- Considering q_j, the change in C_B can not be occurred by manipulating q_j which is the jacket flowrate.

- Other inputs can be analyzed by the open loop responses asfollows:

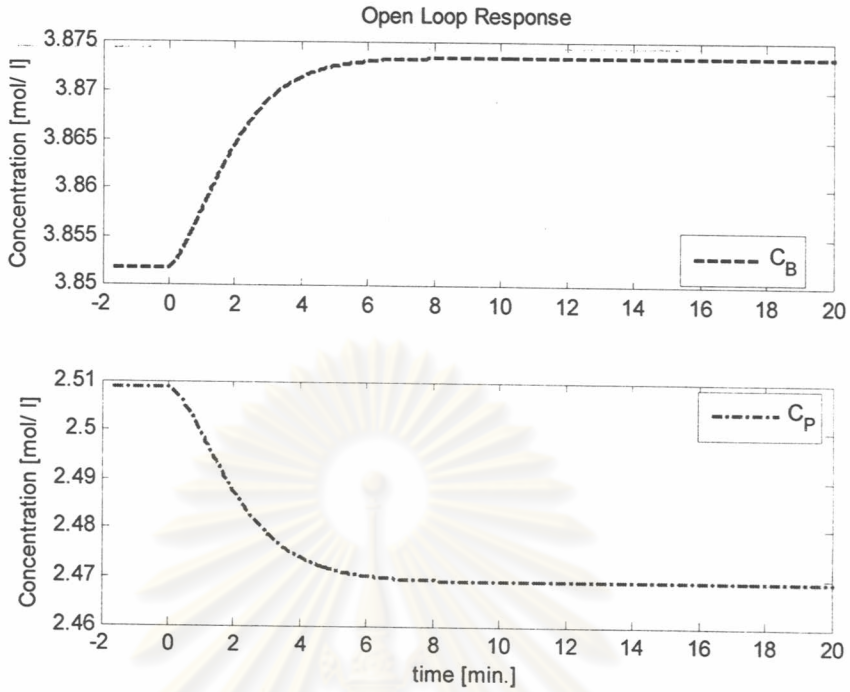

Figure 4.2: Process Dynamics Response of C_{Ain} step change -10%

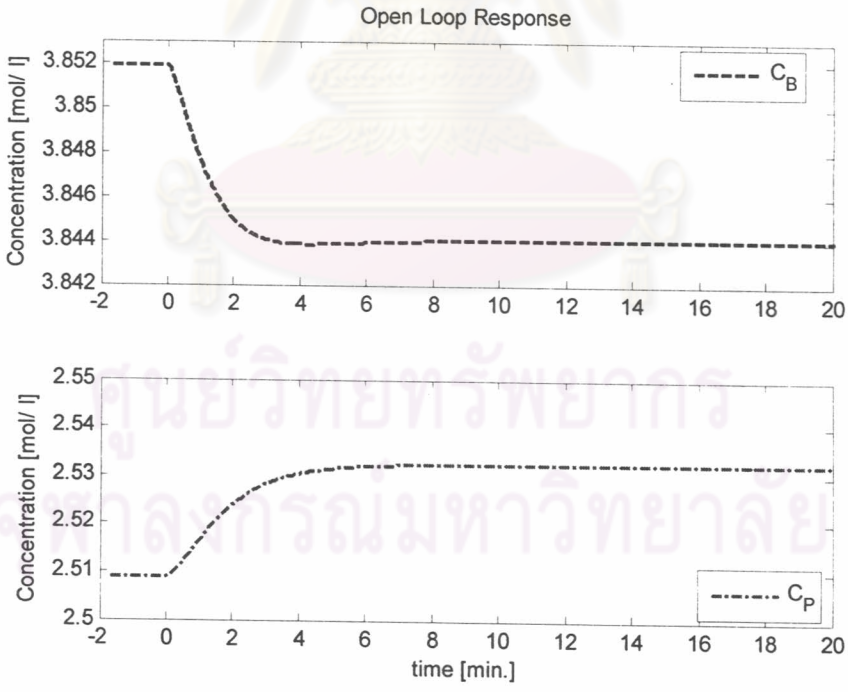

Figure 4.3: Process Dynamics Response of C_{Ain} step change +10%

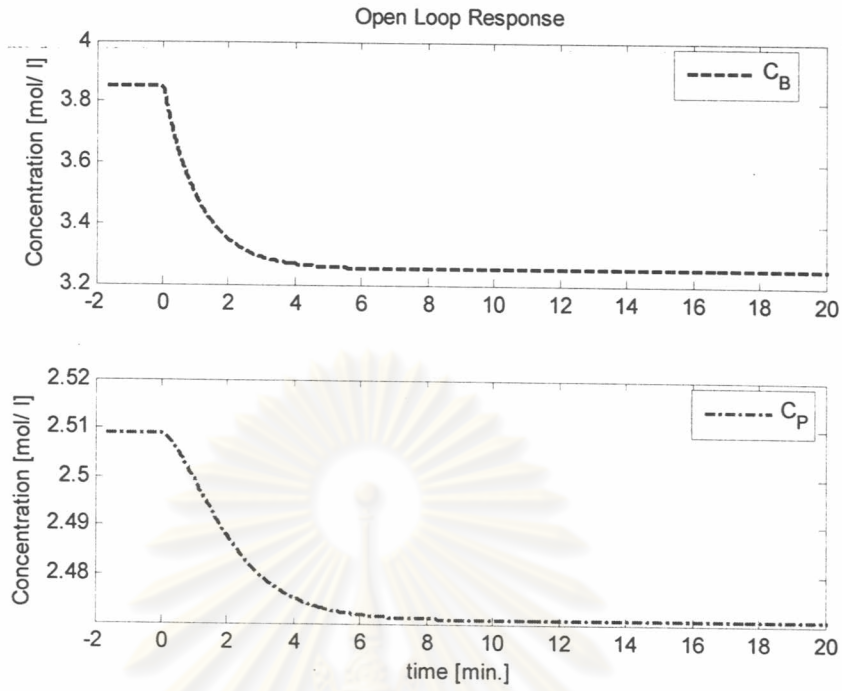

Figure 4.4: Process Dynamics Response of C_{Bin} step change -10%

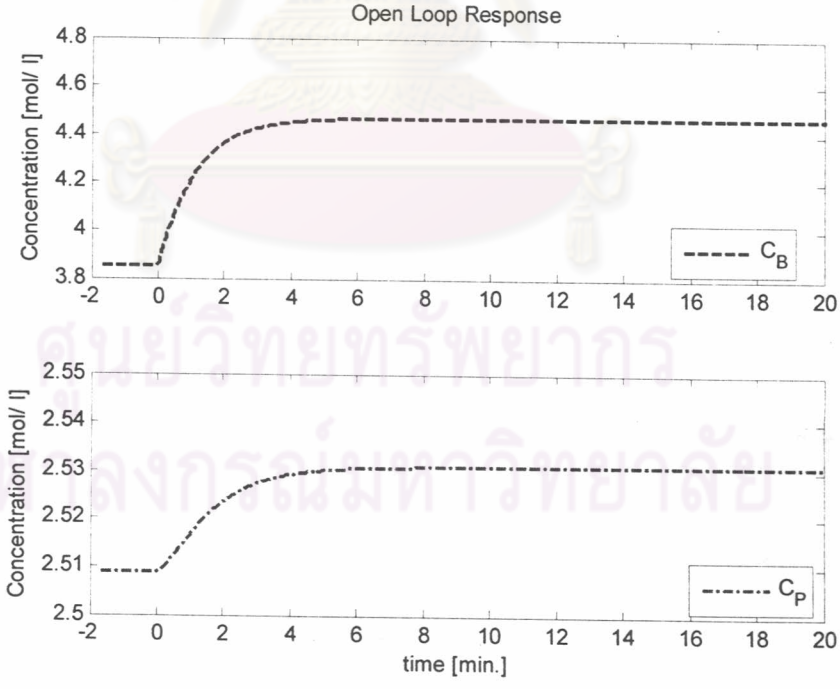

Figure 4.5: Process Dynamics Response of C_{Bin} step change +10%

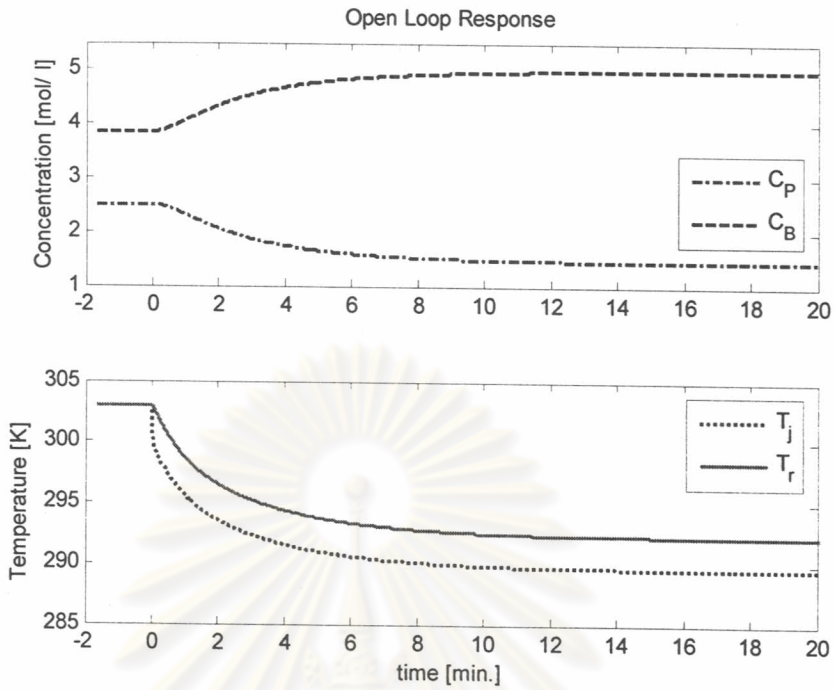

Figure 4.6: Process Dynamics Response of T_j change -10%

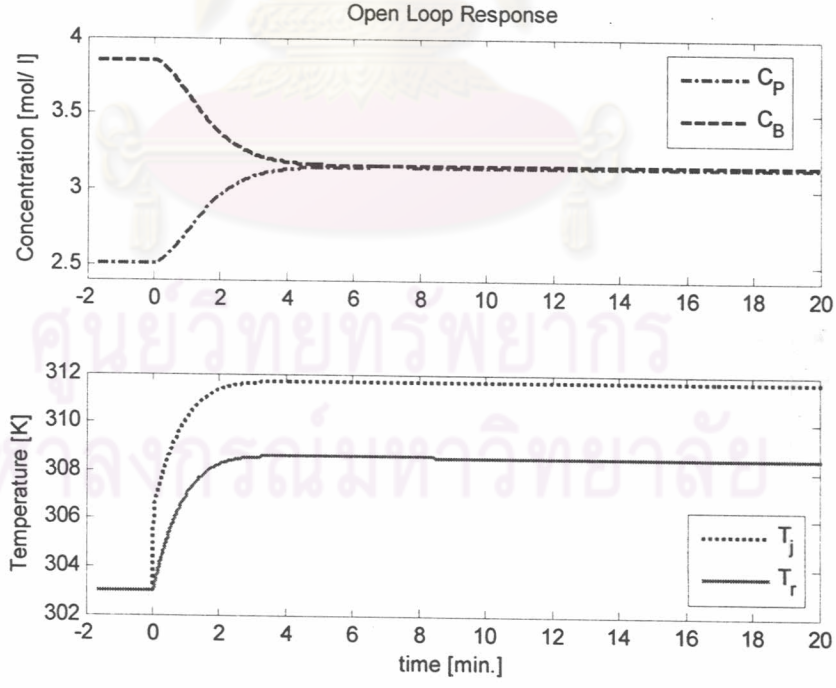

Figure 4.7: Process Dynamics Response of T_j change +10%

From the open loop simulation results, Figure 4.2 shows that a step change of C_{Ain} -10% makes an increase in C_B of about 0.02 kmol/m3 and a decrease in C_P of about 0.04 kmol/m^3. Figure 4.3 shows that a step change of C_{Ain} +10% makes a decrease in C_B of about 0.01 kmol/m3 and an increase in C_P of about 0.02 kmol/m^3, these indicate that the changes of C_{Ain} has only a small effect on the controlled variable and the desired product. Figure 4.4 shows that a step change of C_{Bin} -10% makes an decrease in C_B of about 0.6 kmol/m^3 and a decrease in C_P of about 0.04 kmol/m^3. Figure 4.5 shows that a step change of C_{Bin} +10% makes an increase in C_B of about 0.6 kmol/m^3 and an increase in C_P of about 0.02 kmol/m^3, these indicate that the changes of C_{Bin} has a great effect on the controlled variable but it has only a small effect on the desired product. Figure 4.6 shows that a step change of T_{jsp} -10% makes a decrease in T_j of about 13K, and a decrease in T_r of about 10K, an increase in C_B of about 1.0 kmol/m^3 and a decrease in C_P of about 1.0 kmol/m^3. Figure 4.7 shows that a step change of T_{jsp} +10% makes an increase in T_j of about 9K, and an increase in T_r of about 5K, an decrease in C_B of about 0.8 kmol/m^3 and a increase in C_P of about 0.7 kmol/m^3. Figure 4.6 and Figure 4.7 indicate that the changes of T_j have the greatest effects on the controlled variable and the desired product, and those changes are related to the control objective, therefore, T_j can be used as an appropriate manipulated variable for this process.

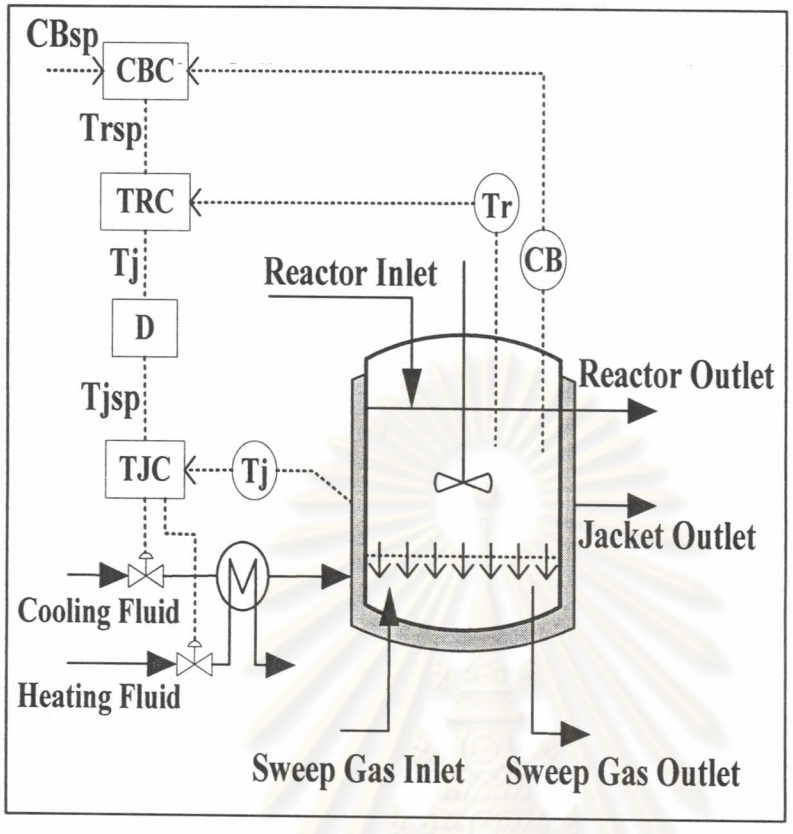

Figure 4.8: Cascade Control Configuration for Etherification Hybrid Process

To achieve an efficient production, the systems need to be controlled. In this research, the cascade control strategies were utilized to control this etherification hybrid process. Disturbances arising within the secondary loop are corrected by the secondary controller before they can affect the value of the primary controlled output which is the main controlled variable of the processes. The cascade control configuration for etherification hybrid process is shown in Figure 4.8. The primary controlled variable, CB, is measured and sent to the primary controller, CBC, which also receives the primary command signal, CBsp, then calculates the secondary command signal, Trsp, and sends it to the secondary controller, TRC. TRC also receives the measured process signal, Tr, and calculates the manipulated variable, Tj, and sends it to the jacket temperature controller. Considering the dynamics of Tj, if Tj is applied directly as the set point for jacket temperature control system, the result in control response would be sluggish. To accommodate such an effect, it is reasonable to

assume that the dynamics of the jacket control system can be approximated by the first order model (Liptak, 1986), as follows:

$$T_{jsp}(k) = T_j(k-1) + \frac{V_j\left(T_j(k)-T_j(k-1)\right)}{q_j \bullet \Delta t} \tag{4.21}$$

The dynamics of Tj can be compensated by the equation above which is the dynamic compensator, D, as shown in Figure 4.8. This Tjsp is the command signal sent to the jacket temperature controller, TJC, through a heat exchanger system opens or closes control valves reflecting to the flow rate of heating and cooling fluid.

4.3 Neural Network Modeling

There are two purposes of neural network models in this work, the Forward Model for using as an internal model and the Inverse Model for using as a controller in the Nonlinear Internal Model Control (NIMC) strategy. The training and testing data sets for the neural network model are generated from the obtained white box mathematical model. The data needs to be normalized for achieving a good performance neural network model. Also, the data normalization requires the maximum and minimum values of each variable. During the off-line training, the whole data sets for each variable from every time step were used simultaneously. In this case, the maximum and minimum values are available from various time steps. But for the on-line implementation, the data sets from only the past and current time steps are available and the maximum and minimum values in the future are unknown. In this research, the manipulated variable (T_j) constraints are 363 K and 293 K. And for the temperature data (T_j and T_r), 373 K and 273 K were used as the maximum and minimum values for data normalization respectively. The equations for data normalization and converting back can be expressed as follows:

$$y = (x-273) / (373-273) \tag{4.22}$$

$$x = y*(373-273) + 273 \tag{4.23}$$

where, y is the normalized value and x is the actual value.

The training data and testing data were generated by the various amplitudes of excited step inputs. The excitation frequencies using are 1/300 Hz for forward model training and 1/90 Hz for inverse model training. Three different sets of data were generated, two for training and one for testing. The temperatures data signal, T_r and T_j, were collected by using the same sampling time of 10 sec, the concentration data signal, C_B, was collected by using the sampling time of 120 sec. The training was done by the Levenberg-Marquardt algorithm using the "early stopping method". The Mean Square Error (MSE) value is the criterion for network selection and also for stopping weights and biases adjustment. During the training, the neural network is still adjusting the weights and biases in each node connections, but there was no adjustment during the testing to evaluate the neural network performance. The details of neural network training have been described previously in CHAPTER III.

4.3.1 Neural Network Forward Model

The Neural Network Forward Model which represents the forward dynamics of the plant is composed of five input nodes, seven nodes for both hidden layers with the log-sigmoid transfer functions and one output node with a linear transfer function, or [5-7-7-1] architecture. The Forward Model represents a future value of T_r which can be expressed as a function of current values of T_j and T_r, two past values of T_j and one past value of T_r as follows:

$$T_r^{(k+1)} = f(T_r^{(k)}, T_r^{(k-1)}, T_j^{(k)}, T_j^{(k-1)}, T_j^{(k-2)}) \qquad (4.24)$$

Where, *k* denotes the current time step of the variables.

The criteria for choosing the neural network inputs are described as follows:

- When an input is removed from the input data set, if the network performance goes worse, that input is required for modeling, and if the network performance does not go worse, that input can be removed from the data set.

- For a dynamic system modeling, it typically requires the current and past values of the corresponding future prediction values which are the controlled variable values for the field of process control. Thus there are the current and past values of T_r in the input data set for this work.

- In this work, the modeling is purposed for NIMC strategy. Therefore, the manipulated variable values are required for the forward modeling, purposed for the inverse model to calculate the manipulated variable and send the control signal to the final control element when implemented.

The neural network forward model is selected by the following procedure using MSE as performance index:

1. The first guess using 5 nodes for both first and second hidden layers [5-5-5-1]. The result is shown in Figure 4.9, MSE = 4.22×10^{-5}.

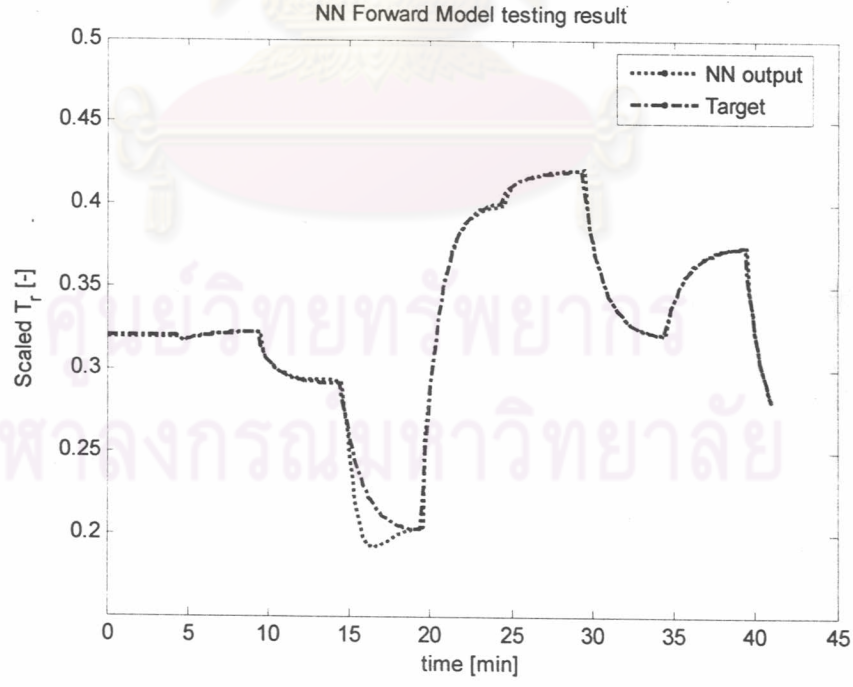

Figure 4.9: NN Forward Model Testing Result [5-5-5-1]

Figure 4.9 shows that the network has underfit on the training data, the network response is too less complex, because the network has too less number of neurons. Thus, the number of neurons should be increased.

2. The second guess was done using 9 nodes for both first and second hidden layers [5-9-9-1]. The result is shown in Figure 4.10, MSE = 8.21×10^{-5}.

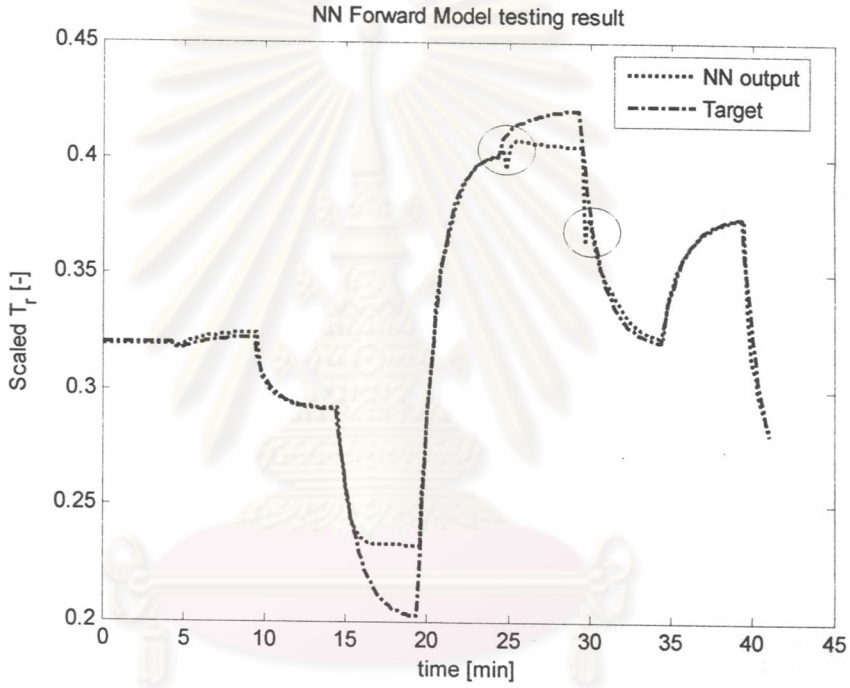

Figure 4.10: NN Forward Model Testing Result [5-9-9-1]

An overfit response is shown in Figure 4.10, as in the circles, the response is oscillated with more frequency than the excitation frequency, the network response is too much complex, because the network has too much number of neurons. Thus, the number of neurons should be decreased.

3. The appropriate number of neurons in the hidden layers should lies between 5, 5 and 9, 9, the comparison was done by using the MSE values as performance index as follows:

S1	S2	MSE	S1	S2	MSE	S1	S2	MSE
5	5	4.22×10^{-5}	7	5	0.0558	9	5	0.0150
5	7	0.0025	7	7	8.36×10^{-6}	9	7	3.71×10^{-4}
5	9	7.68×10^{-5}	7	9	9.98×10^{-5}	9	9	8.21×10^{-5}

Table 4.1: Neural Network Forward Model Architectures Comparison

Where, S_1 is the number of neurons in the first hidden layer

S_2 is the number of neurons in the second hidden layer

As seen from Table 4.1, The chosen architecture is [5-7-7-1] which gave the best modeling performance indicated by the MSE value of 8.36×10^{-6}.

The neural network forward model architecture is shown in Figure4.11.

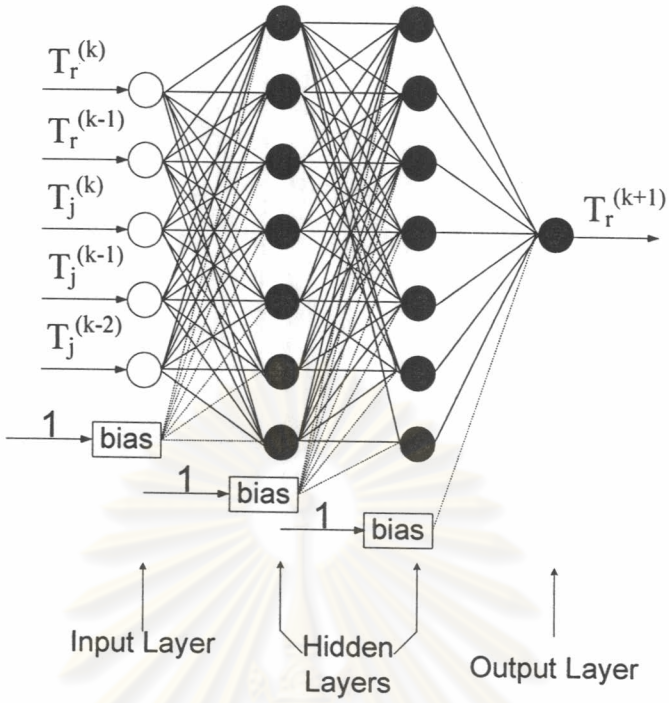

Figure 4.11: Neural Network Forward Model Architecture

4.3.2 Neural Network Inverse Model

The Neural Network Inverse Model which represents the inverse dynamics of the plant is composed of seven input nodes, three nodes for the first hidden layer, three nodes for the second hidden layer with the log-sigmoid transfer function for both hidden layers, and one output node with a linear transfer function, or [7-3-3-1] architecture. The Inverse Model representing the current value of T_j can be expressed as a function of a future, a current and a past value of T_r, two past values of T_j and two past values of C_B with the less sampling frequency than that of T_r and T_j, as follows:

$$T_{jsp}^{(k)} = f^{-1}(T_r^{(k+1)}, T_r^{(k)}, T_r^{(k-1)}, T_{jsp}^{(k-1)}, T_{jsp}^{(k-2)}, C_B^{(k-1)}, C_B^{(k-2)}) \quad (4.19)$$

Where, *k* denotes the current time step of the variables.

The obtained forward model is not one-to-one relation between inputs and output, thus, there is only the pseudo-inverse available which replaces the output of

forward model by the current value of the manipulated variable. The future value of the controlled variable becomes an input and all other values are still the same.

The temperature signals, T_r and T_j, are sampled every 10 sec., while the reactant concentration, C_B, which is also the controlled variable, was added to improve the network control performance by allowing the network to know the value of C_B every 120 sec.

Note that the future value of the output ($T_r^{(k+1)}$) is required in Eq. (4.19). During the off-line training, this value is available, but not for on-line implementation. This value can be replaced by the IMC error, $e^{(k)}$, which is defined as follows:

$$e^{(k)} = T_{rsp}^{(k)} - [T_r^{(k)} - \hat{T}_r^{(k)}] \qquad (4.20)$$

The Neural Network Inverse Model Architecture is also chosen by the same procedure used for the forward model as described before, the results are shown in Table 4.2.

S1	S2	MSE	S1	S2	MSE	S1	S2	MSE
11	0	0.1323	3	3	2.08×10^{-5}	5	3	5.70×10^{-5}
15	0	0.0066	3	5	4.19×10^{-5}	5	5	1.96×10^{-4}
19	0	0.0017						

Table 4.2: Neural Network Inverse Model Architectures Comparison

Where, S_1 is the number of neurons in the first hidden layer

S_2 is the number of neurons in the second hidden layer

The number of neurons in the input and output layers are 7 and 1, respectively, all the same for all architectures.

From Table 4.2, the architecture [7-3-3-1] has the best performance compared with other architectures by the MSE performance index which is equal to 2.08×10^{-5}.

The Neural Network Inverse Model Architecture is shown in Figure 4.12.

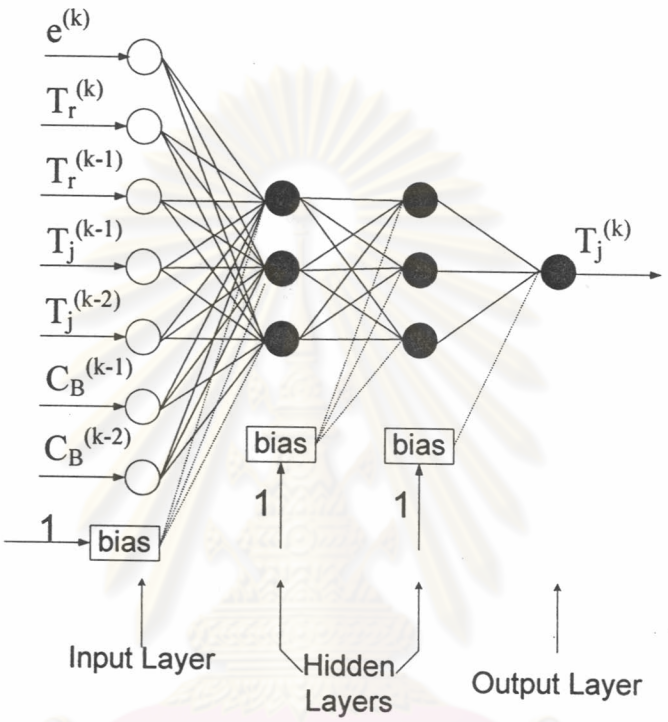

Figure 4.12: Neural Network Inverse Model Architecture

The neural network performance testing result is shown in Figure 4.13.

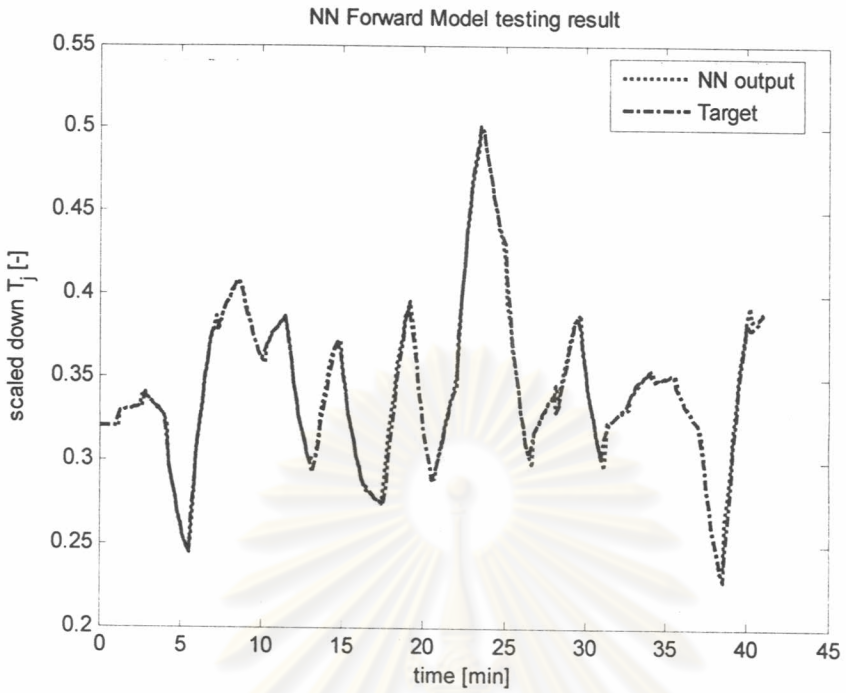

Figure 4.13: Neural Network Inverse Model performance testing result

4.4 Neural Network Control

After the forward and inverse models are obtained, they will be implemented in the PI-NIMC cascade strategy as shown in Figure 4.14 below:

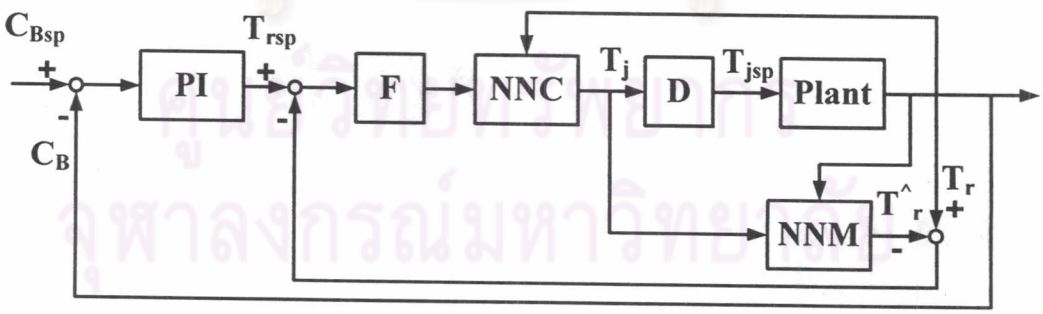

Figure 4.14: PI-NIMC Cascade Topology

Where, F stands for Filter, D stands for Dynamic Compensation, NNC stands for Neural Network Controller placed by the obtained inverse model, NNM stands

for Neural Network Model placed by the obtained forward model and PI is a Proportional Integral Controller.

In this research, a measured reactor temperature (T_r) signal with noise was simulated according to the electrical noise from the electronic measuring instruments. This is a high frequency (every time step of simulation, 0.5 sec.) and low amplitude (±2 K) noise. The exponential filter was implemented prior to the inverse model acting as a controller for the system robustness improvement. The appropriate filter time constant, τ_F, is the minimum value of τ_F that large enough to quarantine the closed loop stability. The filter was tuned based on case 2, τ_F=70 sec. was set. The results of using various τ_F are shown in cases 2 and 3.

Since the plant model and the inverse model are represented by two independently trained different neural networks, the product of steady state gains may not be in unity, therefore leading to some steady state offsets in the controlled variable. For this reason, the PI-NIMC cascade strategy was utilized. As such, the secondary controlled variable (T_r) offset is allowable and the primary controlled variable (C_B) offset is eliminated by the Integral term of PI controller. The PI controller in the hybrid strategy was tuned on-line by by Ziegler-Nichols method of which K_C is equal to -34 and τ_I is equal to 80. The performance of PI-NIMC cascade strategy is compared with that of the conventional PID cascade control. To show a superiority of PI-NIMC cascade strategy, the electrical noise in temperature signals was not applied for PID cascade control, while that was applied for PI-NIMC strategy. The configuration of PID cascade control is shown in Figure 4.15, PID1 is the primary controller and PID2 is the secondary controller. The tuning parameters are; K_{C1} is equal to -1.95 and τ_{I1} is equal to 80 for PID1 without any derivative action, and K_{C2} is equal to 2,200 for PID2 with small integral action, τ_{I2} is equal to 100,000, and no derivative action. Both controllers were set to take control action every 10 sec.

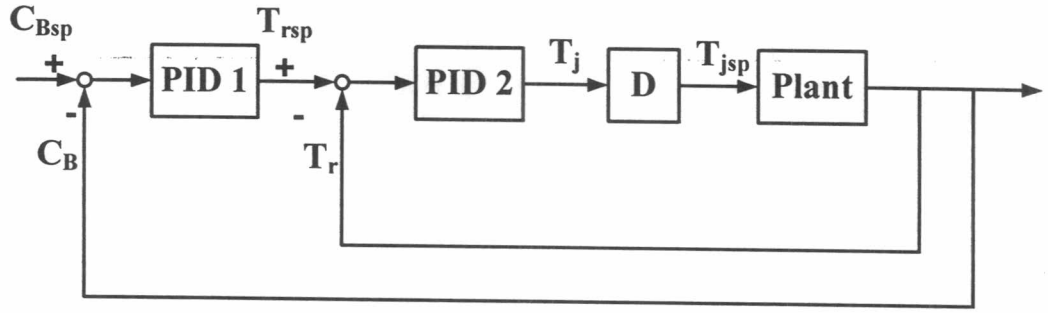

Figure 4.15: PID Cascade Topology

4.5 Closed Loop Simulation Result

In the closed loop simulation studies, the control performance of PI-NIMC cascade strategy (PI-NN) is compared with the conventional PID cascade control (PI-P) in cases of disturbances rejection and plant-model mismatches conditions. All changes of disturbances and mismatches were introduced at the time, t = 0 minute. The Integral of Absolute Error (IAE) and the Integral of Time-weighted Absolute Error (ITAE) were utilized as the control performance indices. The simulation results are shown as follows:

4.5.1 Case 1: nominal case

In this case, the set point, C_{Bsp}, was decreased 30% from the nominal operating condition. The simulation results are shown in Figure 4.16(a), IAE value given by PI-NN is 266 while that of PI-P is 262. Figure 4.16(a) shows that both controllers gave the same response at the beginning until 2 minutes after the set point change. After that, the responses are different; the response of PI-P has an oscillation while that of PI-NN is more smooth.

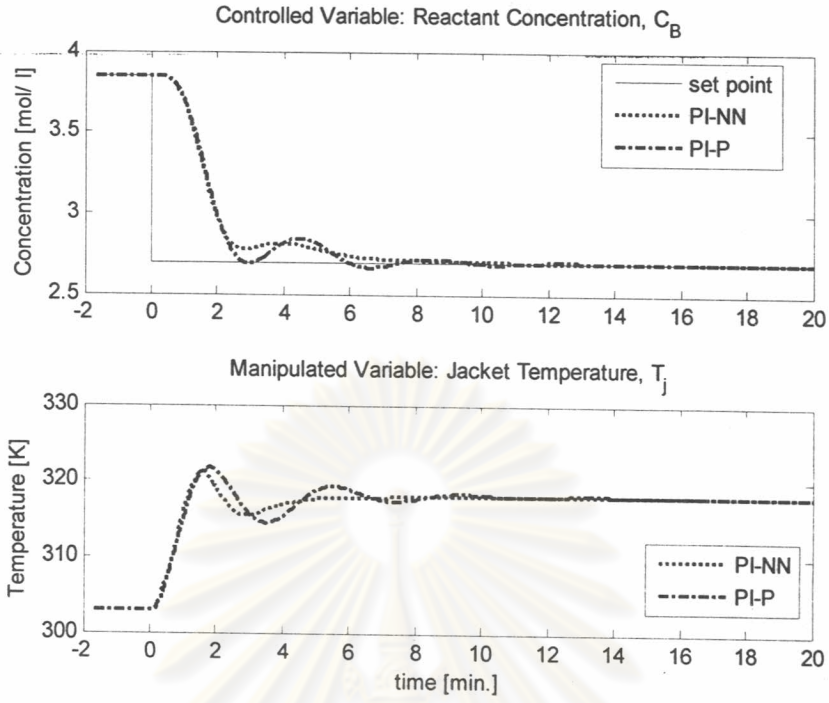

Figure 4.16(a): Nominal Case

For robustness test, the controllers should have an equalized performance in the nominal case. Therefore, PI-P should be retuned to achieve the same value of IAE as given by PI-NN. The retuned parameters of PI-P are; K_{C1}= -1.94, and other parameters are still the same. These parameters are used for all robustness test of PI-P in this research. The simulation results of the nominal case with a retuned PI-P are shown in Figure 4.16(b). The response of PI-P is slower than before, this is related to the decreased performance, indicated by the increased IAE value.

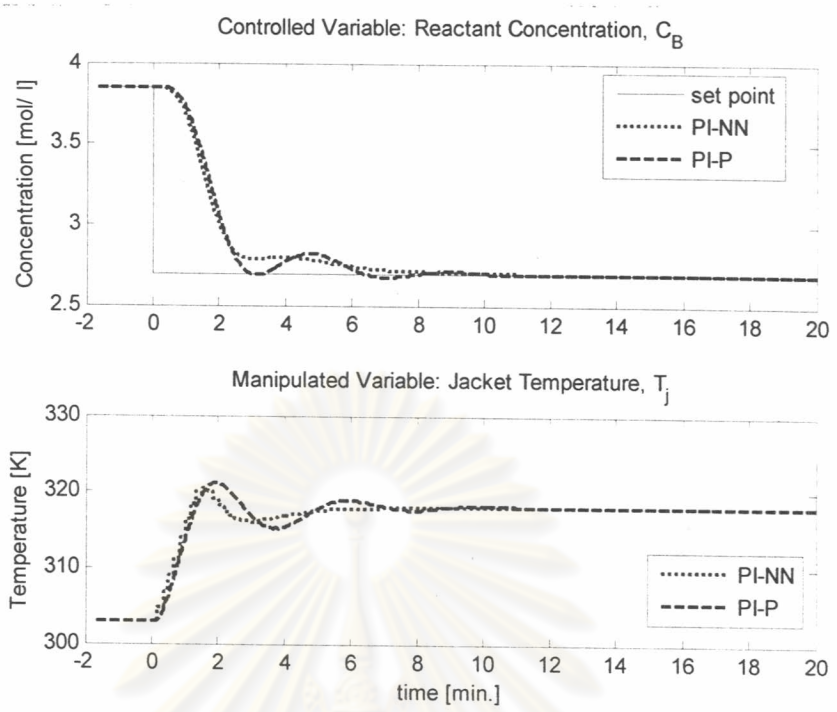

Figure 4.16(b): Nominal Case, retuned PI-P

4.5.2 Case 2: disturbance change, -20% C_{Bin}

The feed concentration, C_{Bin}, was decreased 20% from the nominal operating condition. In this case, the robustness filter, F, has shown a prior role by improving closed loop stability of PI-NN. The simulation results of using various filter time constant, τ_F = 0 (no filtering), 70 and 140 sec., are shown in Figures 4.17(a), 4.17(b) and 4.17(c), respectively.

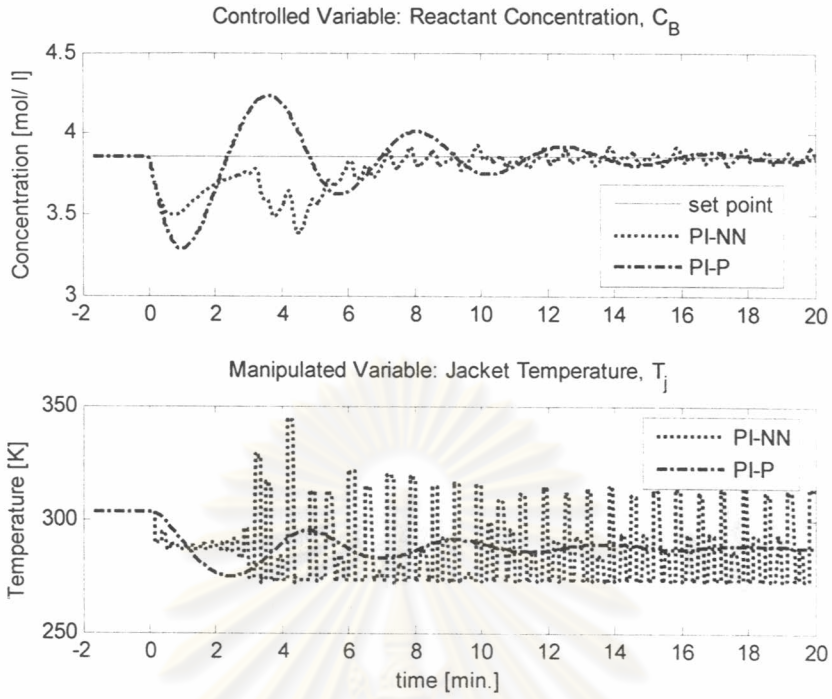

Figure 4.17(a): Disturbance Change, -20% C_{Bin}, τ_F = 0 (no filtering)

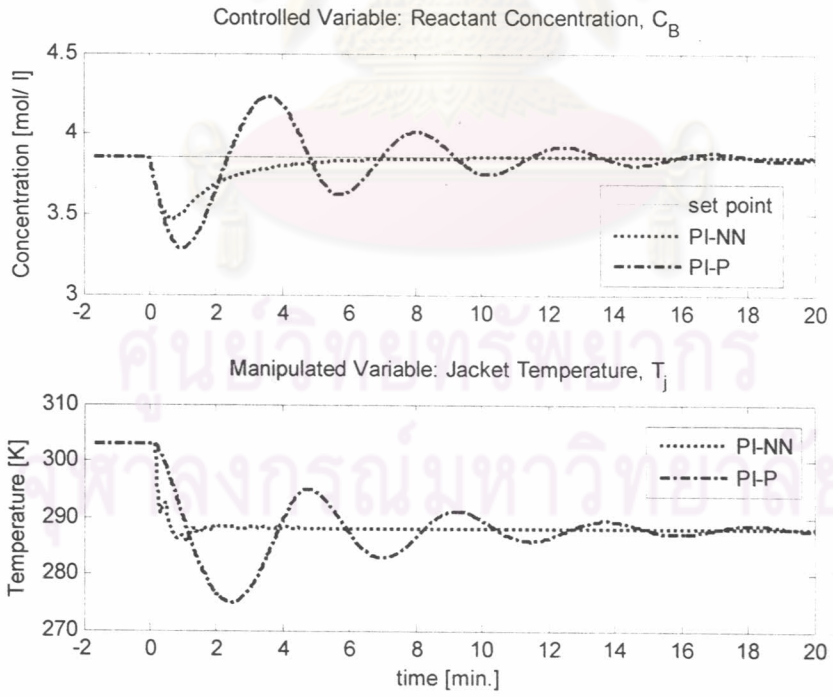

Figure 4.17(b): Disturbance Change, -20% C_{Bin}, τ_F = 70 sec.

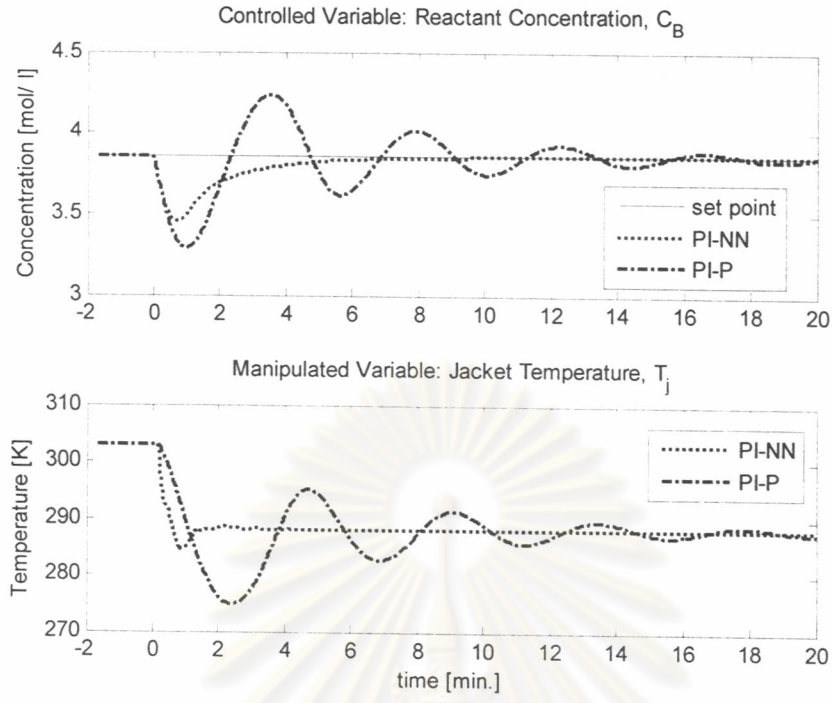

Figure 4.17(c): Disturbance Change, -20% C_{Bin}, τ_F = 140 sec.

Figure 4.17(a) shows an unstable response of PI-NN which can be catered by filtering as shown in Figures 4.17(b) and 4.17(c). The IAE values are shown in Table 4.3. In this case, there is not any significant result between using τ_F of 70 and 140.

Case	IAE				ITAE			
	PI-NN			PI-P	PI-NN			PI-P
	τ_F=0	τ_F=70	τ_F=140		τ_F=0	τ_F=70	τ_F=140	
2. -20% C_{Bin}	219	99	99	283	66,148	11,508	11,348	84,324
3. +20% C_{Bin}	91	100	109	139	10,047	10,913	12,326	20,054

Table 4.3: Comparison of using various τ_F in PI-NN

4.5.3 Case 3: disturbance change, +20% C_{Bin}

The feed concentration, C_{Bin}, was increased 20% from the nominal operating condition. In this case, it was found that the response of PI-NN is stable even without filtering as shown in Figure 4.18(a). Moreover, the response gets slower when τ_F is increased as seen from Figures 4.18(a), 4.18(b) and 4.18(c), and as seen in Table 4.3 that IAE and ITAE values are increased.

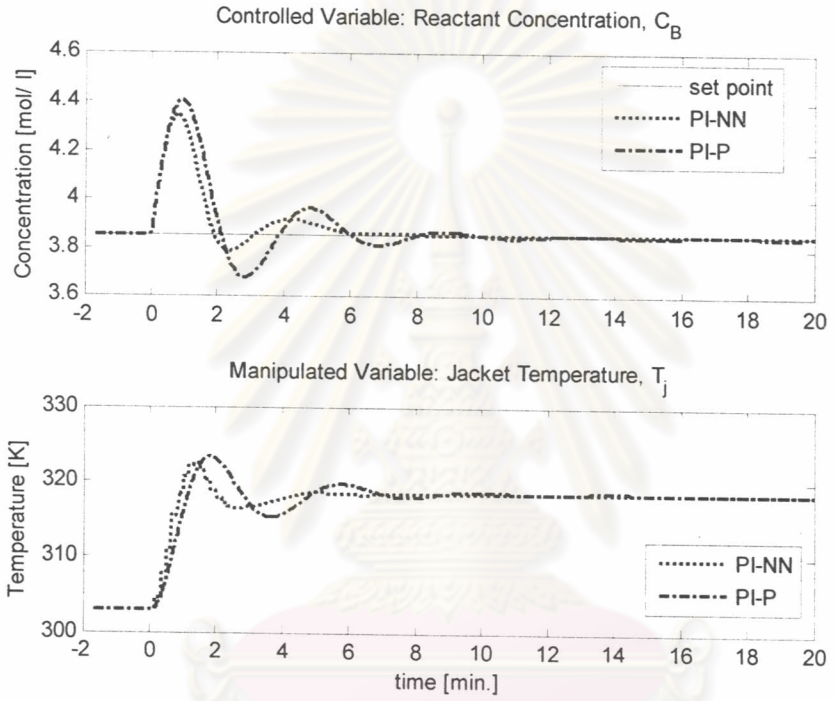

Figure 4.18(a): Disturbance Change, +20% C_{Bin}, $\tau_F = 0$ (no filtering)

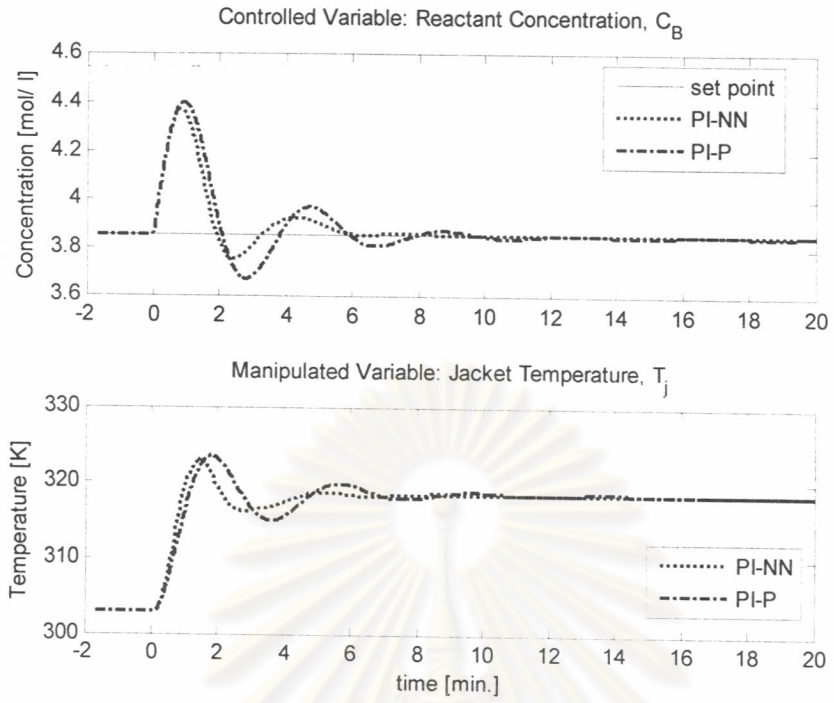

Figure 4.18(b): Disturbance Change, +20% C_{Bin}, $\tau_F = 70$

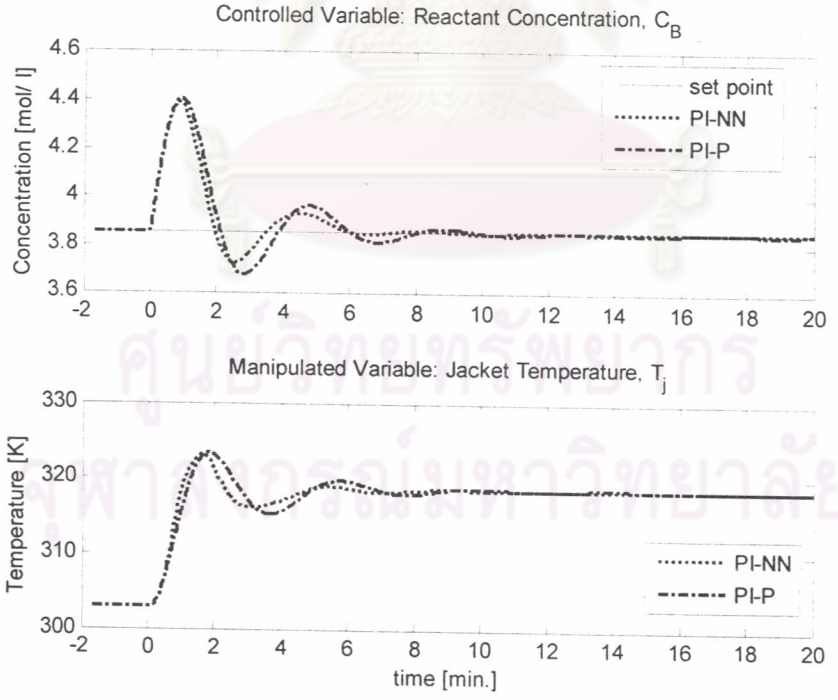

Figure 4.18(c): Disturbance Change, +20% C_{Bin}, $\tau_F = 140$

In the following cases 4 to 9, the robustness test of PI-NN was done using τ_F = 70 only.

4.5.4 Case 4: disturbance changes, -20K T_F

The feed temperature, T_F, was decreased 20K from the nominal operating condition. The results are shown in Figure 4.19.

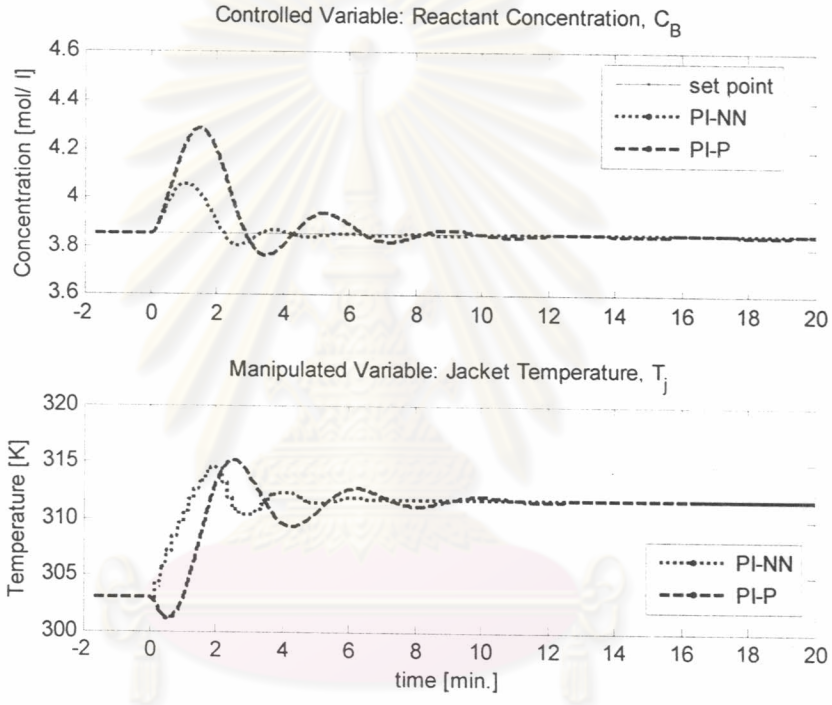

Figure 4.19: Disturbance Change, -20K T_F

The IAE values are 39 for PI-NN and 118 for PI-P. The ITAE values are 3,612 for PI-NN and 19,144 for PI-P. As seen in Figure 4.19, the control action of PI-P was taken with the wrong direction in the beginning, this is the cause of large error given from PI-P while PI-NN took the correct direction and gave smaller error.

4.5.5 Case 5: disturbance changes, +20K T_F

The feed temperature, T_F, was increased 20K from the nominal operating condition. The results are shown in Figure 4.20.

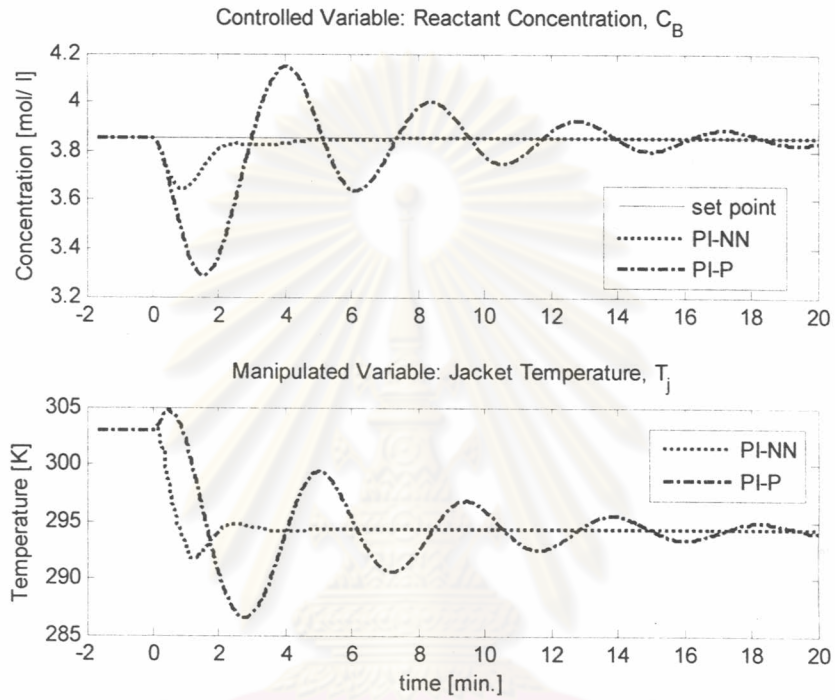

Figure 4.20: Disturbance Change, +20K T_F

The IAE values are 39 for PI-NN and 273 for PI-P. The ITAE values are 3,819 for PI-NN and 87,584 for PI-P. Similar to case 4, the control action of PI-P was taken with the wrong direction in the beginning. Moreover, PI-NN gave a smooth and stable response while PI-P gave an unstable response.

4.5.6 Case 6: plant-model mismatch, -30% k_1

The reaction rate constant, k_1, was decreased 30% from the nominal operating condition. The results are shown in Figure 4.21.

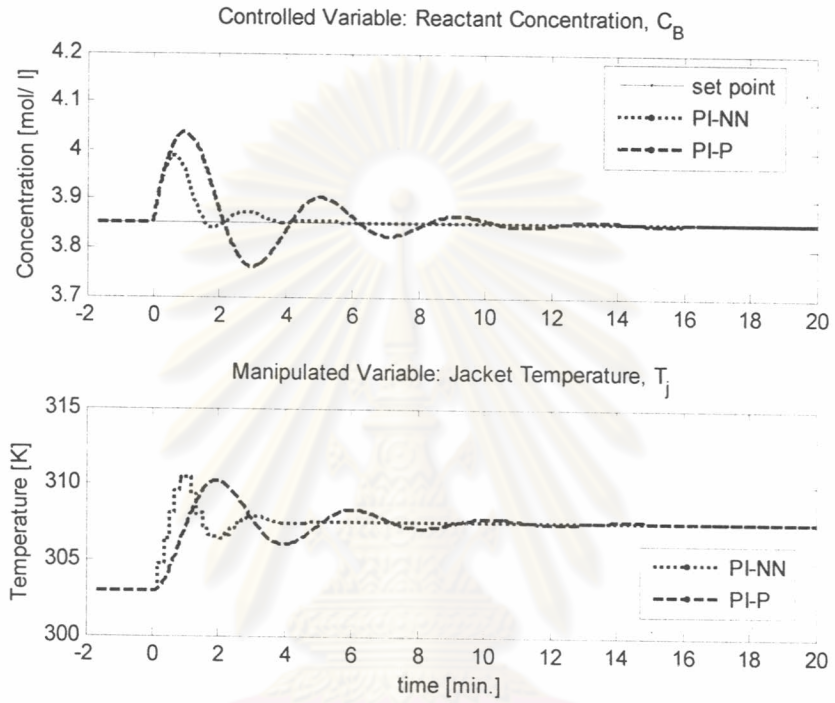

Figure 4.21: Plant-Model Mismatch, -30% k_1

The IAE values are 19 for PI-NN and 61 for PI-P. The ITAE values are 1,417 for PI-NN and 11,935 for PI-P. As seen from Figure 4.21, the response of PI-NN is more drastic and more stable than that of PI-P.

4.5.7 Case 7: plant-model mismatch, +30% k_1

The reaction rate constant, k_1, was increased 30% from the nominal operating condition. The results are shown in Figure 4.19.

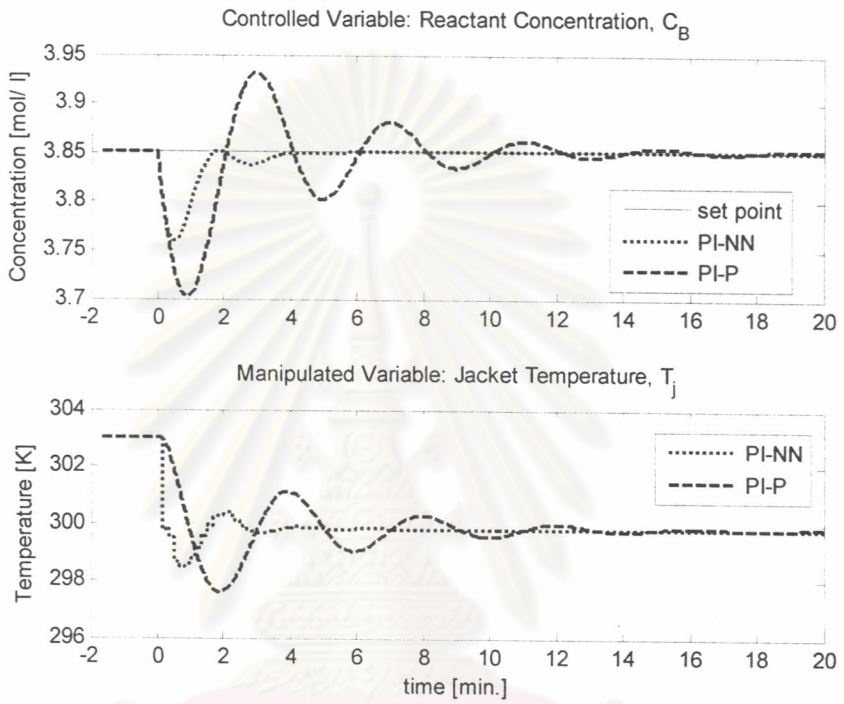

Figure 4.19: Plant-Model Mismatch, +30% k_1

The IAE values are 13 for PI-NN and 54 for PI-P. The ITAE values are 988 for PI-NN and 12,104 for PI-P. Similar to case 6, the response of PI-NN is more drastic and more stable than that of PI-P.

4.5.8 Case 8: plant-model mismatch, -30% k_2

The reaction rate constant, k_2, was decreased 30% from the nominal operating condition. The results are shown in Figure 4.20.

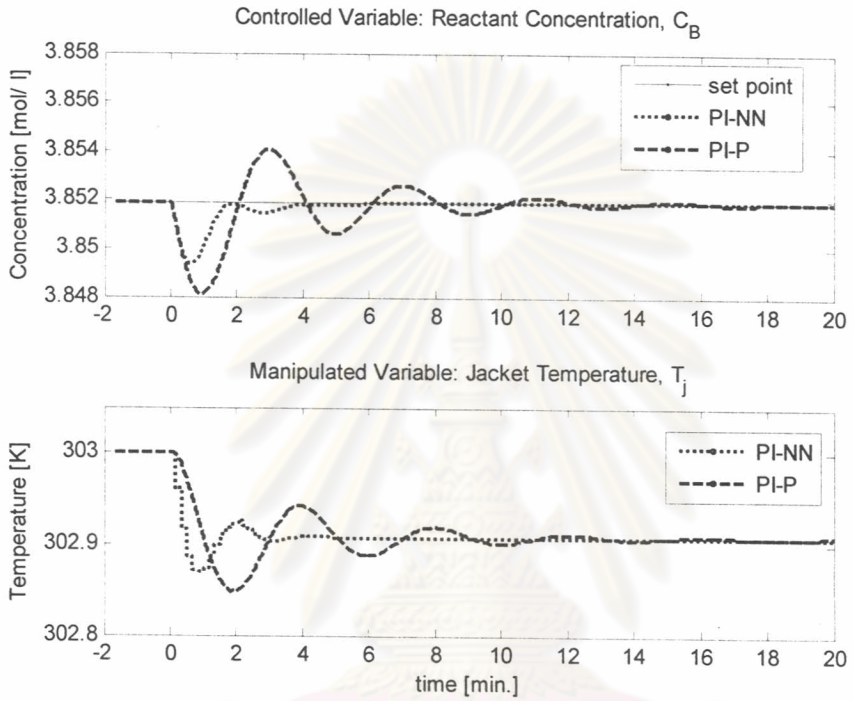

Figure 4.20: Plant-Model Mismatch, -30% k_2

The IAE values are 0.31 for PI-NN and 1.37 for PI-P. The ITAE values are 31 for PI-NN and 304 for PI-P. Similar to cases 6 and 7, the response of PI-NN is more drastic and more stable than that of PI-P.

4.5.9 Case 9: plant-model mismatch, +30% k_2

The reaction rate constant, k_2, was increased 30% from the nominal operating condition. The results are shown in Figure 4.21.

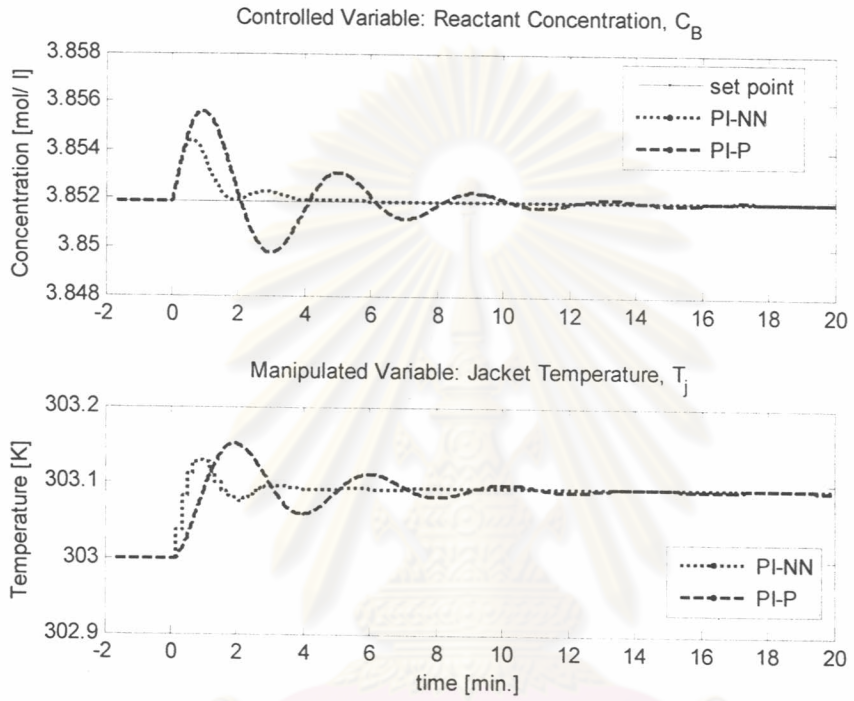

Figure 4.20: Plant-Model Mismatch, -30% k_2

The IAE values are 0.37 for PI-NN and 1.38 for PI-P. The ITAE values are 31 for PI-NN and 292 for PI-P. Similar to cases 6, 7 and 8, the response of PI-NN is more drastic and more stable than that of PI-P.